REGULAR PAPER

First insights into the vertical habitat use of the whitespotted eagle ray *Aetobatus narinari* revealed by pop-up satellite archival tags

Lauran R. Brewster[1] | Brianna V. Cahill[1] | Miranda N. Burton[1] |
Cassady Dougan[1] | Jeffrey S. Herr[1] | Laura Issac Norton[1] |
Samantha A. McGuire[1] | Marisa Pico[1] | Elizabeth Urban-Gedamke[1] |
Kim Bassos-Hull[2] | John P. Tyminski[2] | Robert E. Hueter[2] |
Bradley M. Wetherbee[3,4] | Mahmood Shivji[4] | Neil Burnie[5] | Matthew J. Ajemian[1]

[1]Harbor Branch Oceanographic Institute, Florida Atlantic University, Fort Pierce, Florida

[2]Sharks and Rays Conservation Research Program, Mote Marine Laboratory, Sarasota, Florida

[3]Department of Biological Sciences, University of Rhode Island, Kingston, Rhode Island

[4]The Guy Harvey Research Institute, Nova Southeastern University, Dania Beach, Florida

[5]Bermuda Shark Project, Bermuda

Correspondence
Lauran R. Brewster, Fisheries Ecology and Conservation Lab, Harbor Branch Oceanographic Institute, 5600 US-1 North, Fort Pierce, FL, 34946, USA.
Email: lbrewster@fau.edu

Funding information
Bermuda Zoological Society; Guy Harvey Ocean Foundation

Abstract

The whitespotted eagle ray *Aetobatus narinari* is a tropical to warm-temperate benthopelagic batoid that ranges widely throughout the western Atlantic Ocean. Despite conservation concerns for the species, its vertical habitat use and diving behaviour remain unknown. Patterns and drivers in the depth distribution of *A. narinari* were investigated at two separate locations, the western North Atlantic (Islands of Bermuda) and the eastern Gulf of Mexico (Sarasota, Florida, U.S.A.). Between 2010 and 2014, seven pop-up satellite archival tags were attached to *A. narinari* using three methods: a through-tail suture, an external tail-band and through-wing attachment. Retention time ranged from 0 to 180 days, with tags attached *via* the through-tail method retained longest. Tagged rays spent the majority of time (82.85 ± 12.17% S.D.) within the upper 10 m of the water column and, with one exception, no rays travelled deeper than ∼26 m. One Bermuda ray recorded a maximum depth of 50.5 m, suggesting that these animals make excursions off the fore-reef slope of the Bermuda Platform. Individuals occupied deeper depths (7.42 ± 3.99 m S.D.) during the day *versus* night (4.90 ± 2.89 m S.D.), which may be explained by foraging and/or predator avoidance. Each individual experienced a significant difference in depth and temperature distributions over the diel cycle. There was evidence that mean hourly depth was best described by location and individual variation using a generalized additive mixed model approach. This is the first study to compare depth distributions of *A. narinari* from different locations and describe the thermal habitat for this species. Our study highlights the importance of region in describing *A. narinari* depth use, which may be relevant when developing management plans, whilst demonstrating that diel patterns appear to hold across individuals.

KEYWORDS

Bermuda, biotelemetry, diel vertical migration, elasmobranch, Gulf of Mexico, PSAT

1 | INTRODUCTION

Mobile marine species often exhibit complex horizontal and vertical movements. Understanding both movement patterns is critical to revealing a species' behaviour and ecology, including foraging, reproduction, habitat use and human interactions (Cooke et al., 2012; Hays et al., 2015). Whilst historically challenging to observe, the development of biologging and biotelemetry technology has offered great insight into how organisms use the marine environment (Hays et al., 2015; Hussey et al., 2015; Sequeira et al., 2019). Data derived from these devices have provided opportunities to assess ecosystem connectivity and develop conservation and management practices (Braun et al., 2014; Cooke et al., 2012; Hays et al., 2015). In particular, knowledge of a species' preferred location in the water column can help reduce vulnerability to human threats, such as fishing or boat strikes, and can promote a better understanding of its ecological role, for example in benthic-pelagic coupling (Braun et al., 2014; Cooke, 2008).

Our understanding of pelagic batoid habitat use is relatively limited due to the transient nature of these species and the challenges associated with capturing and tagging them. Fortunately, recent applications of biologging and biotelemetry technology have facilitated some initial insights into the behaviour of these elusive species. For example, research on the reef manta ray Manta alfredi (Krefft 1868), a planktivorous coastal-pelagic batoid, indicates that patterns of vertical movement vary by location. M. alfredi in the British Indian Ocean Territory exhibit diel vertical migration (DVM), occupying deeper mean diving depths during the day and moving up through the water column at night (Andrzejaczek et al., 2019), whilst in the Red Sea and around the Seychelles M. alfredi remain closer to the surface during the day and dive deeper at night (Braun et al., 2014; Peel et al., 2020), a movement pattern known as reverse DVM. Both vertical movement strategies may be driven by foraging behaviour, with the contrasting patterns being attributed to regional oceanography affecting the distribution of their prey (Andrzejaczek et al., 2020). DVM patterns have also been observed in more benthic batoids such as the short-tail stingray Bathytoshia brevicaudata (Hutton 1875) (Le Port et al., 2008) and several skate species (Humphries et al., 2017; Wearmouth & Sims, 2009). However, DVMs exhibited by benthic species may represent nektobenthic displacement (i.e., inshore/offshore movement along the substrate; Humphries et al., 2017) rather than a change in position in the water column as observed in more pelagic animal DVMs. Nonetheless, foraging strategies are also thought to be a dominant driver for benthic species' DVMs (Humphries et al., 2017; Le Port et al., 2008; Wearmouth & Sims, 2009).

Not all batoids demonstrate diurnal patterns of vertical habitat use and other biotic and abiotic factors beyond foraging can explain dive behaviour. For example, the cownose ray Rhinoptera bonasus (Mitchill 1815), a benthopelagic schooling ray, exhibited no diel differences in depth or temperature but rather depth use varied between sexes and across seasons as feeding habitats changed with migration (Omori & Fisher, 2017). Temperature has been coined the "ecological master factor" that affects the physiology of aquatic ectotherms and consequently many fish, including the bat ray Myliobatis californica Gill 1865, behaviourally thermoregulate (Brett, 1971; Matern et al., 2000). Lunar phase, due to its relationship with tides, illumination and changes in predator–prey distribution, has also been shown to influence the depth and habitat use of several elasmobranch species (Braun et al., 2014; Dewar et al., 2008; Vianna et al., 2013; Whitty et al., 2017), including M. alfredi (Braun et al., 2014; Peel et al., 2020). Additional investigation into the vertical movement of batoids and the reasons for these movements could shed light on potential interactions between species and trophic dynamics (Vaudo et al., 2014). However, despite the importance of understanding vertical movements to elucidate the ecology of a species, little is known about this behaviour in many large marine species, such as the whitespotted eagle ray Aetobatus narinari (Euphrasen 1790).

A. narinari is a large batoid ray inhabiting the subtropical and tropical coastal waters of the western Atlantic Ocean (Naylor et al., 2012; Richards et al., 2009; White et al., 2010). There are conservation concerns for A. narinari; the International Union for the Conservation of Nature (IUCN) classifies the species as Near Threatened due to its life history characteristics, marketability and accessibility using inshore fishing gear (Kyne et al., 2006). As such, the species is afforded protection in parts of its range, including Florida and Alabama state waters, around the Islands of Bermuda, the Maldives and the Great Barrier Reef, Australia. The species is highly mobile, with tagged individuals showing movements of 258.1 km (±23.9 S.E.; DeGroot, 2018), and has a demonstrated genetic link between populations in Florida and Cuba (Sellas et al., 2015). Despite its migratory potential, A. narinari is known to exhibit high levels of multiyear philopatry (Ajemian et al., 2012; Bassos-Hull et al., 2014; Cerutti-Pereyra et al., 2018; DeGroot, 2018; Flowers et al., 2017). As a benthopelagic mesopredator, like R. bonasus, A. narinari forms an important link between benthic and pelagic environments (Ajemian et al., 2012; Serrano-Flores et al., 2019) and could play an important role in bioturbation (O'Shea et al., 2012).

Vertical movements of A. narinari have only been described in a few short-term studies. In Bimini, Bahamas, diel movements were correlated with tidal phase; individuals aggregated to refuge in three deeper core areas during low tide (Silliman & Gruber, 1999). In Bermuda, Ajemian et al. (2012) identified diel patterns in depth use by A. narinari in Harrington Sound, a semi-enclosed inshore lagoon accessible to the open ocean via a single inlet. Similar movement patterns on the surrounding reef were inferred from Smart Positioning and Temperature (SPOT) satellite tag transmissions (Ajemian & Powers, 2014). However, taken together, these studies were unable to provide fine-scale depth data outside of Harrington Sound, limiting our understanding of how A. narinari uses deeper habitats beyond inshore sounds of the Bermuda Islands.

The goals of this study were to use pop-up satellite archival tags (PSATs) to (a) quantify A. narinari vertical habitat use; (b) investigate the influence of environmental drivers known to affect depth use in other batoids; and (c) examine the effect of two different locations—Florida, USA and the Islands of Bermuda—with different habitat characteristics (continental shelf and bay/insular shelf respectively).

Knowledge of the vertical movement patterns of *A. narinari* will help provide a more cohesive understanding of overall habitat use and behavioural trends, which can be used to inform future management in countries where this species remains vulnerable to human threats.

2 | MATERIALS AND METHODS

2.1 | Capture and tagging techniques

Seven *A. narinari* were fitted with PSATs (Table 1), five near Sarasota, FL, U.S.A. (Figure 1) with Standard rate X-Tags (Microwave Telemetry, Inc., Columbia, MD, U.S.A.; 122 × 33 mm, weight in air = 46 g), and two near Bermuda (Figure 1) with MiniPAT tags (Wildlife Computers Inc., Redmond, WA, U.S.A.; 124 × 38 mm, weight in air = 60 g). Programmed tag detachment ranged from 120 to 270 days (Table 1). All Sarasota tags had archived and transmitted sampling rates of 2 and 15 min, respectively. The animals in Sarasota were captured and tagged in September of 2010, October of 2010 and May of 2013. The Bermuda rays had archived and transmitted sampling rates of 5 s and 5 min, respectively. Animals in Bermuda were caught and tagged in August of 2014.

Rays were caught with either a 500 × 4 m nylon seine net in Sarasota or a 100 × 5 m purse seine net in Bermuda. Capture involved visually spotting a ray in shallow water (<4 m), encircling with the respective nets, reducing net compass size and using a smaller scoop net to transfer the animal onto the boat. For rays caught in Sarasota, each individual was placed into a livewell on the boat with a free-flowing bilge pump supplying ambient, oxygenated seawater. Animals from Sarasota were sampled and tagged while in the livewell. For the individuals caught in Bermuda, each ray was placed on the deck of the boat with a hose into the buccal cavity to actively pump water over the gills. A towel was placed over the eyes to minimize stress during transit back to the Bermuda Aquarium for tagging. For the tagging procedure, the ray was transferred to a land-based clove oil bath for sedation (25 mg l^{-1}) (Grusha, 2005). At both tagging locations rays were measured (disc width, cm), sexed and fitted with a PSAT; however, tag attachment varied among individuals (Table 1).

The absence of prominent structures and strong tissue in rays can make the attachment and retention of animal-borne devices difficult (Ward *et al.*, 2019), a problem that may be further aggravated for batoids like *A. narinari* that breach (Silliman & Gruber, 1999). Consequently, in this study three techniques were explored for PSAT attachment (Table 1 and Figure 2). The first technique was the through-wing method (Figure 2a) which involved inserting a hollow tagging needle (cleaned with 70% alcohol) from the ventral side through the caudal part of the pectoral fin. Monofilament (136 kg test), looped through the base of the PSAT, was passed into the hollow needle from the anterior side and both the needle and monofilament were pulled back through to the ventral side. The monofilament was secured with a steel fishing crimp on either side of the wing. To provide a more secure attachment point and reduce abrasion from the crimp, a soft, tear-resistant pad (made of polyester-reinforced PVC pool liner bonded with 1/8″ inch neoprene) was placed between the animal and the crimp, on either side of the wing. Excess monofilament on the ventral side was trimmed prior to release. This attachment method was used to tag two Sarasota rays (S1 and S3; Table 1). The second technique was the tail-band method (Figure 2b), which was applied for Sarasota rays S2 and S4. The tail-band was constructed using a plastic cable tie encased in plastic tubing that was large enough to fit around the widest part of the base of the tail. The tail-band contained a small loop to pass a second small cable tie through to connect to the PSAT. The third technique, the through-tail suture, was used for the final Sarasota ray (S5) and both Bermuda rays. The through-tail method involved using a stainless-steel needle (cleaned with 70% alcohol) to pass either a wire tie in black poly-tubing (S5) or aircraft cable encased in silastic tubing (40.8 kg test; Bermuda rays) through the musculature at the base of the tail and crimping it back on itself on the dorsal side, creating a bridle to which the PSAT was attached (Figure 2c; see Le Port *et al.*, 2008). Heat-shrink tubing was heated over the crimps to minimize abrasion and the possibility of predation from the reflective metal acting like a fishing lure.

Tag attachment times varied by method; the through-wing method was the fastest (~6 min), followed by the tail-band (~10 min). The through-tail method took the longest at ~20 min. Following tag attachment, Bermuda rays were moved from the anaesthesia tank to

TABLE 1 Tag deployment and individual biometric data for *A. narinari*, including disc width (DW), type of data and sampling frequency used for analysis, monitoring period (*i.e.*, intended attachment duration) and actual retention duration

| Ray ID | DW (cm) | Sex | Tagging date | Tagging location | | Attachment method | Data retrieved | Data interval | Monitoring period (days) | Retention period (days) |
				Lat.	Lon.					
S1	150	F	28 September 2010	27.267	−82.570	Through-wing	Did not report	—	120	—
S2	150	F	7 October 2010	27.267	−82.570	Tail-band	Archive	—	120	<1
S3	151	F	14 October 2010	27.267	−82.570	Through-wing	Did not report	—	270	—
S4	168	M	19 October 2010	27.324	−82.591	Tail-band	Transmit	15 min	180	4
S5	162	F	23 May 2013	27.267	−82.570	Through-tail	Archive	2 min	180	69
B1	127	M	19 August 2014	32.334	−64.727	Through-tail	Transmit	5 min	180	180
B2	110	F	22 August 2014	32.333	−64.728	Through-tail	Archive	5 s	180	97

Note: All Sarasota rays (S1–S5) were fitted with Microwave Telemetry X-Tags and Bermuda animals (B1 and B2) were fitted with Wildlife Computer MiniPAT tags. See text for description of attachment methods.
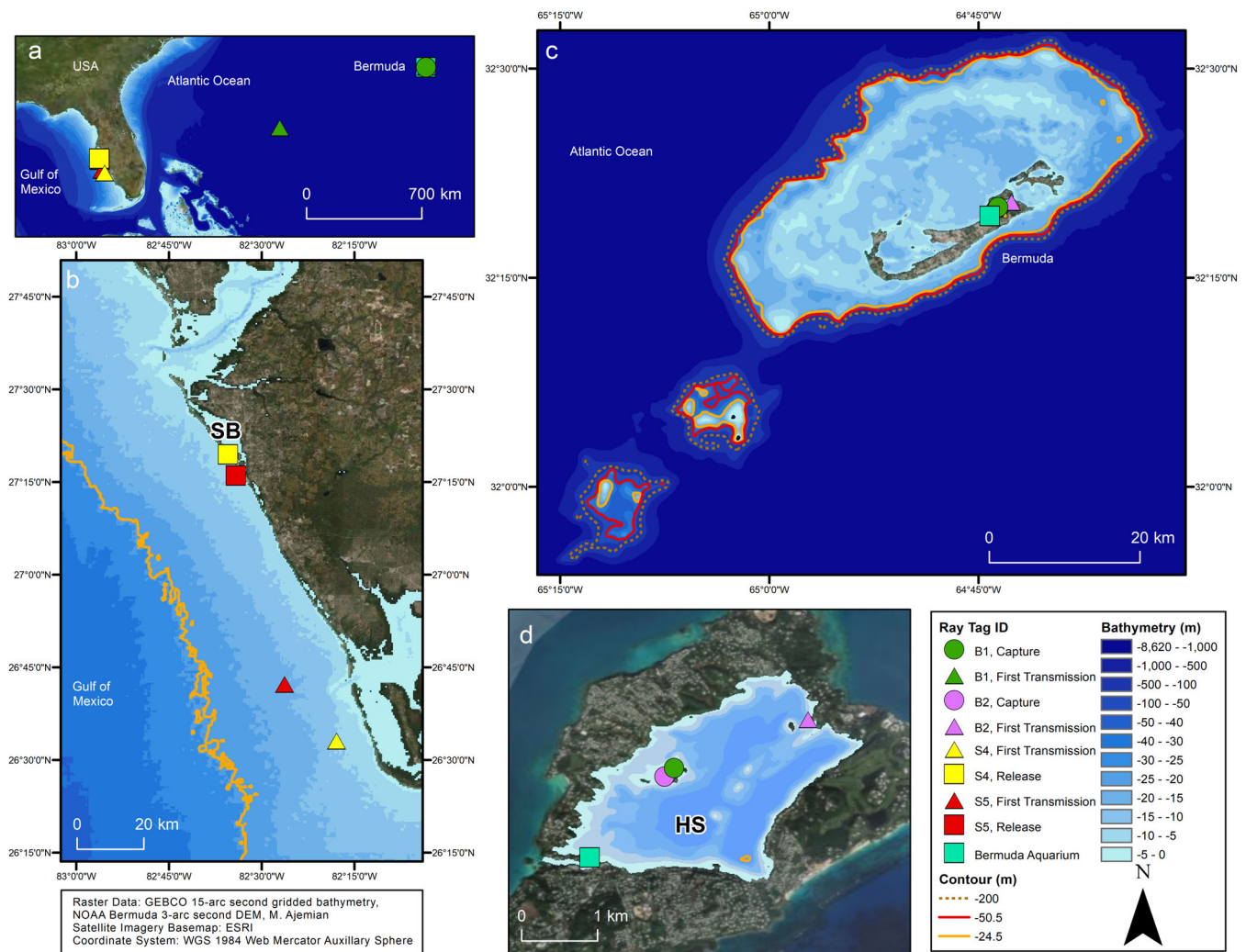
FIGURE 1 Bathymetry map showing capture, release and first pop-up satellite transmission locations of tagged *A. narinari* off Sarasota, Florida, U.S.A. and Bermuda. Capture locations are represented by circles, release locations are represented by squares, whilst triangles represent the first transmission locations (Ray B1, green; Ray B2, purple; Ray S4, yellow; Ray S5, red). (a) The location of the Islands of Bermuda in the western North Atlantic Ocean in relation to Sarasota, off the west coast of Florida, U.S.A. (b) A zoomed in map of S4 and S5 release and first transmission locations as well as Sarasota Bay (SB). (c) The Bermuda Pedestal including the Islands of Bermuda atop the Bermuda Platform and the Challenger and Plantagenet Banks 27 and 41 km to the south-west of Bermuda, respectively. (d) Harrington Sound (HS), an inshore sound largely landlocked by Main Island but connected to the open ocean by Flatts Inlet to the south-west. The release location (Bermuda Aquarium) of the Bermuda rays is indicated by the square. Bathymetry is represented in all maps by blue cells with 24.5 m (solid orange; maximum depth by Sarasota ray S5), 50.5 m (solid red; maximum depth by Bermuda ray B1) and 200 m (dotted orange) depth contours indicated. Note there is one area (Devil's Hole) in Harrington Sound where depth >24.5 m

a recovery tank with ambient seawater to assess their health prior to release at the Bermuda Aquarium dock. Sarasota rays were assessed in the livewell on the boat and released close to the capture location.

2.2 | Ethical statement

All animal handling procedures were approved through Mote Marine Laboratory's IACUC permits #10-03-PH1 and 13-02-PH1, FWC Special Activity Licence (SAL-10-1140-SRP and SAL-13-1140-SRP) and Bermuda Department of Conservation Services permit #14-06-15-06.

2.3 | Data analyses

Satellite-transmitted data were downloaded through a CLS America portal. In the event a tag was physically recovered, the archived data were processed using WC-DAP 3.0 (MiniPATs) or returned to Microwave Telemetry (X-Tags) for download (Table 1). Data were inspected for a constant depth value, indicating the tag had detached from the animal (*i.e.*, the end of the retention period; Table 1) and data including and subsequent to that constant depth point were discarded. All vertical movement analyses were conducted in R Core Team (2020). To analyse the horizontal movement of the rays, geolocation analysis
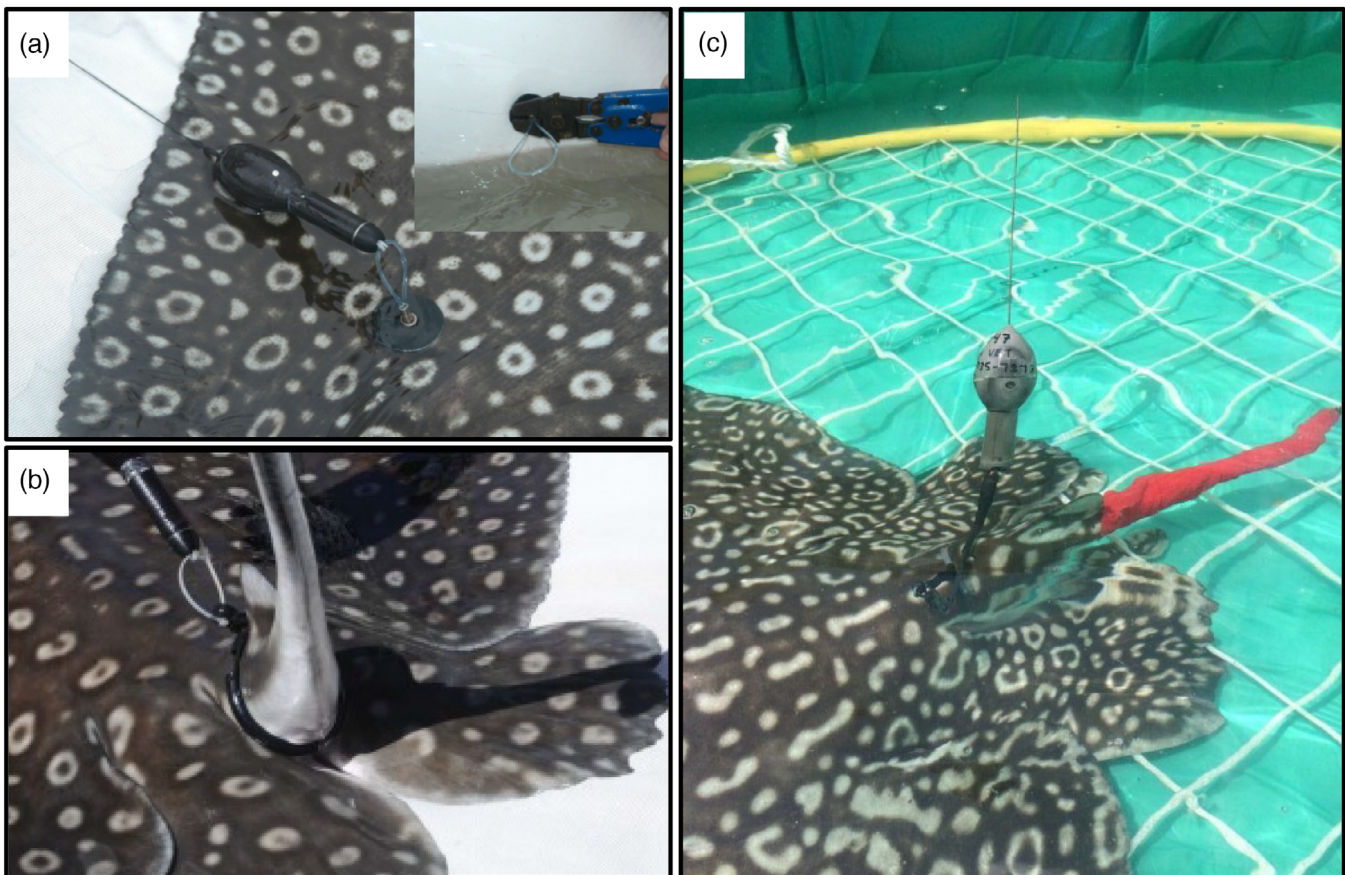
FIGURE 2 Pop-up satellite archival tag (PSAT) attachment methods: (a) through-wing, (b) tail-band and (c) through-tail (see Le Port *et al.*, 2008 for schematic of through-tail attachment method)

was performed for each deployment except S4 because of the short deployment duration. To create maximum likelihood tracks for the Bermuda rays, the MiniPAT data were processed in Wildlife Computers GPE3 software. The program uses the tag data, sea surface temperature (SST) and bathymetric constraints to generate a hidden Markov model that estimates the most likely position of the animal. The model also provides a probability distribution that indicates the quality of the location estimate. To obtain the most probable track for the Microwave Telemetry X-Tag fitted to S5, the data were processed in R using a state-space unscented Kalman filter in the "UKFSST" package (Nielson et al., 2009) along with Reynolds optimally interpolated SST data. Following state-space estimation, we used the "analyzepsat" package to apply a secondary bathymetric correction that constrained estimated locations based on the daily maximum depths that the ray achieved (Galuardi, 2012).

To assess whether depth and ambient temperature (as measured by the tag) distribution varied between night and day for each ray, we conducted Kolmogorov–Smirnov (K-S) tests ($P < 0.001$). The data were identified as "day" or "night" based on sunrise and sunset times obtained from the "suncalc" package (Thieurmel & Elmarhraoui, 2019) at each animal's release location.

To determine the effect of abiotic factors on *A. narinari*, we aggregated the data to calculate hourly means and built a generalized additive mixed model (GAMM) with a gamma distribution to describe mean hourly depth (m). The GAMM was built using the "mgcv" package (Wood, 2006). GAMMs are a semiparametric approach used for modelling effects in response to a variety of predictor variables simultaneously and can account for repeated measures and serial correlation (Hastie & Tibshirani, 1990). Abiotic factors considered included tagging location (Sarasota/Bermuda), hour of the day, month, moon phase and SST (°C). Moon phase [0.0–1.0; representing new moon, waxing crescent, first quarter, waxing gibbous, full moon (0.5), waning gibbous, last quarter and waning crescent] was extracted using the "suncalc" package. Hourly SST was derived as the mean temperature when the animal was within 5 m of the surface (Andrzejaczek *et al.*, 2018). As part of data exploration prior to model development, we plotted the response variable against each covariate, investigated potential interactions and assessed collinearity between covariates using conditional boxplots and generalized variance-inflation factor (GVIF) scores; covariates yielding GVIF values higher than 3 were removed and scores were recalculated (Zuur *et al.*, 2009, 2010). Circular smoothers were applied to hour of the day and moon phase. Smoothing splines were automatically optimized using cross-validation in the "mgcv" package (Wood, 2006). Ray ID was added to the model as a random effect to avoid pseudo-replication and account for individual variation. An auto-correlation plot was used to assess if

there was serial correlation between residuals where a value at time t is a linear function of the value at $t-1$ (Zuur et al., 2009). The auto-correlation plot indicated temporal correlation was evident in the initial model residuals and thus an auto-regressive process of order 1 was included. To balance model fit with model size, Akaike Information Criterion (AIC; Akaike, 1973) scores were used for optimal model selection. The model with the lowest AIC score was selected unless a more parsimonious model had an AIC value within two of the lowest score (Burnham & Anderson, 2002). Models were validated by examining routine diagnostics (Q-Q plots, histograms of residuals, response versus fitted values and linear predictors versus residuals).

3 | RESULTS

Four of the seven deployed tags successfully transmitted and/or archived data (Table 1). S1 and S3 did not report, and one tag (S2) was recovered after washing ashore. S2 demonstrated regular vertical movements for approximately 2 h, at which point the tag was either ensnared at depth (and detached) or the animal died and sank to the bottom (tag remaining attached). Of the remaining four A. narinari, tag retention periods varied between 4 days (S4) up to the programmed duration of 180 days (B1; Table 1). Early detachment of the tags from S4 and B2 occurred because the tag's constant depth release mechanism was triggered. Examination of the tag's tether revealed that a slipped crimp caused the early release from S5. All four tags transmitted data via the ARGOS satellites; two of these were recovered and the full datasets accessed (B2 and S5). The Sarasota rays' (S4 and S5) distance between release locations and first satellite transmissions were 101 and 72 km, respectively (Figure 1). Similarly, for the Bermuda A. narinari (B2), the first transmitted detection was in close proximity to the release location; however, the other Bermuda ray (B1) first transmitted ~990 km away from its release location, 107 days after the tag release from the animal (Figure 1).

The results of the geolocation analyses for S5, B1 and B2 were considered unrepresentative of the horizontal movements exhibited by the three rays and are consequently not presented. Typical geolocation accuracy for both the X-Tag and MiniPAT are ±1° latitude, ±0.5° longitude but PSAT estimates of geolocation using light-based methods can be associated with large margins of error in cases where there is not much overall tag displacement (Braun et al., 2015; Brunnschweiler et al., 2010; Hueter et al., 2018; Omori & Fisher, 2017), as was the case for B2 and S5. For B1, although it clearly moved over deep water (see below), the late report confounded the pop-off location and thus confidence in the track was low.

3.1 | Depth distribution

Bermuda A. narinari experienced a wider range of depths than those tagged off Sarasota, with one ray reaching a maximum depth of 50.5 m. The two Sarasota rays were found at depths <25 m for the entire tracking period (Table 2 and Figure 3). Bermuda rays also occupied a deeper mean depth (Table 2). All rays spent the majority of the time (82.85 ± 12.17% S.D.) within 10 m of the surface but demonstrated oscillatory diving behaviour throughout the diel cycle (Figure 3). The depth distribution of each individual was significantly different between night and day (B1: $D = 0.19$, $P < 0.001$; B2: $D = 0.41$, $P < 0.001$; S4: $D = 0.34$, $P < 0.001$; S5 $D = 0.19$, $P < 0.001$), with rays consistently occupying shallower mean depths at night (collectively mean day depth = 7.42 ± 3.99 m S.D. vs. mean night depth = 4.90 ± 2.89 m S.D.; Table 2 and Figure 4). There was variability in depth distribution across individuals, but all individuals spent the largest proportion of night-time in the top 10 m of the water column (B1 73.00%, B2 83.07%, S4 100.00%, S5 93.84%).

Apart from one dive to 31 m on 24 August 2014, B1 did not reach depths greater than 25 m until 20 November 2014, approximately

TABLE 2 Mean (±S.D.), depth (m) and temperature (°C) recorded by pop-up satellite archival tags for the four A. narinari

Depth (m)

Ray ID	Overall mean (±S.D.)	Overall range	Day mean (±S.D.)	Day range	Night mean (±S.D.)	Night range
B1	9.51 (± 10.65)	0.50–50.50	10.42 (± 9.65)	0.50–49.50	8.80 (± 11.30)	0.50–50.50
B2	8.23 (± 8.64)	0.00–26.00	11.29 (± 8.76)	0.00–26.00	5.35 (± 7.45)	0.00–25.50
S4	3.14 (± 2.68)	0.00–13.45	3.72 (± 2.56)	0.00–13.45	2.44 (± 2.74)	0.00–8.07
S5	3.71 (± 3.61)	0.00–24.54	4.25 (± 3.89)	0.00–22.86	3.00 (± 3.08)	0.00–24.54

Temp (°C)

Ray ID	Overall mean (±S.D.)	Overall range	Day mean (±S.D.)	Day range	Night mean (±S.D.)	Night range
B1	24.14 (± 3.49)	18.10–32.50	24.52 (± 3.55)	18.10–32.50	23.89 (±3.42)	18.10–29.30
B2	26.33 (± 2.32)	21.50–32.00	26.49 (± 2.30)	21.55–32.00	26.18 (±2.34)	21.50–30.50
S4	24.78 (± 0.17)	24.25–25.30	24.82 (± 0.19)	24.25–25.30	24.73 (± 0.12)	24.43–25.13
S5	29.34 (± 1.44)	25.66–32.86	29.37 (± 1.47)	25.66–32.86	29.31 (± 1.40)	25.66–32.65

Note: Data are given for the overall deployment duration, daytime and night-time along with the respective temperature and depth ranges.
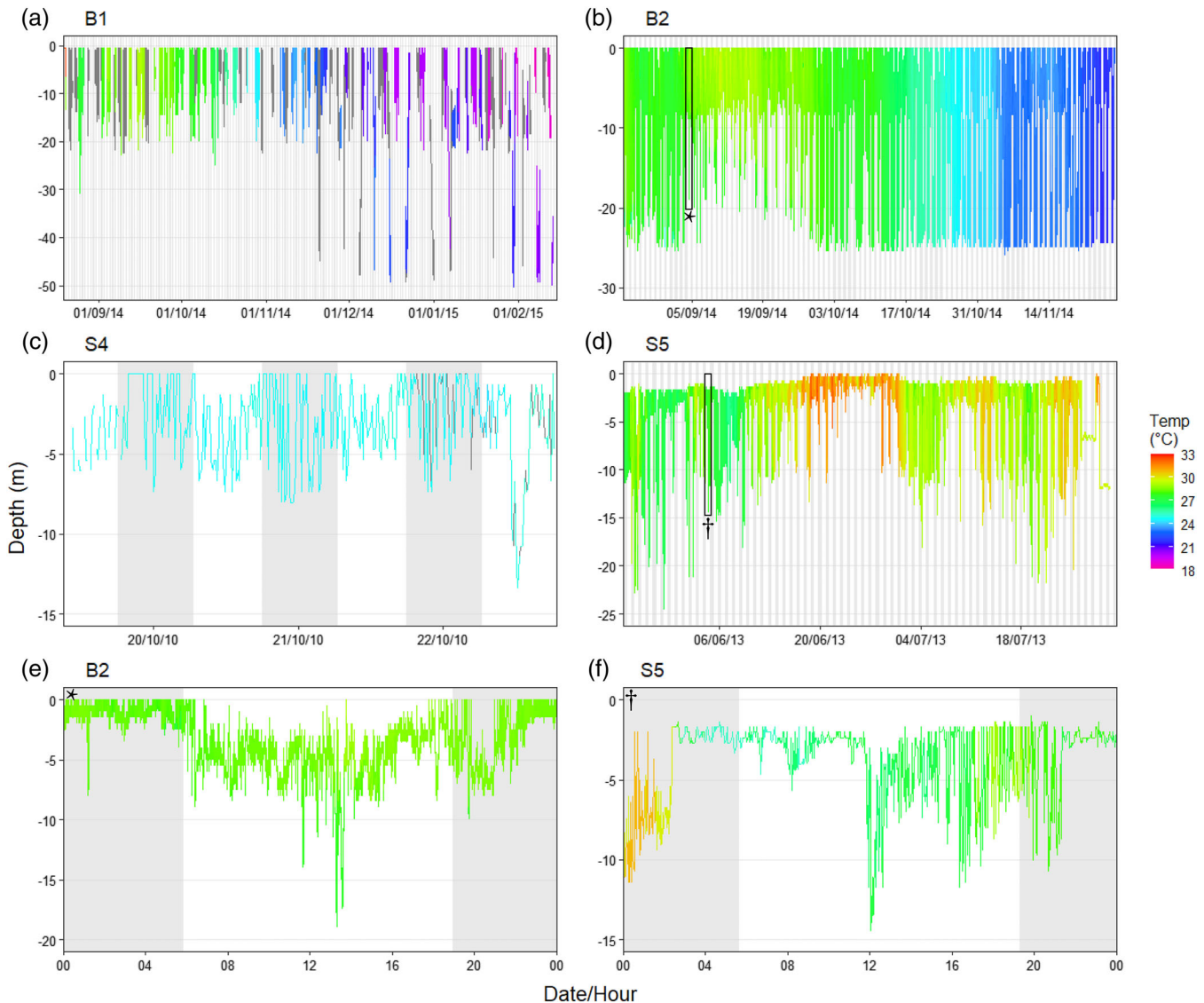
FIGURE 3 Raw temperature (°C) and depth (m) profiles for *A. narinari*. (a)–(d) Profiles for the entire deployment for: (a) B1, transmitted data; (b) B2, archival data; (c) S4, transmitted data; (d) S5, archival data. An example diel period is presented for each archival dataset, (e) B2 and (f) S5, showing oscillatory movements through the water column during both night and day. The diel period selected is indicated by a black box in the respective ray's deployment track. The shaded columns represent night (based on daily sunset and sunrise times at the respective release locations). *Note.* Where temperature data were unavailable, the depth trace is plotted in grey and gaps are present in the transmitted data where data was not retrieved

halfway through the deployment, when surface temperatures dropped below 23°C (Figure 3a). B1 spent 7.41% of the deployment at depths below the 26 m maximum depth obtained by B2. For B2 in particular, depth use was bimodal (Figure 4b). It regularly dove to depths exceeding 20 m throughout the deployment, except during September when water temperature was warmest (Figure 3b). S5 exhibited a similar pattern of shallower depth use (<10 m) with warmer temperatures during late June–early July 2013 (Figure 3d). The deployment of S4 was too short to see discernible changes in depth use over time (Figure 3c).

During data exploration for modelling mean hourly depth using the GAMM, covariates month and SST were found to be collinear and

thus month was omitted from model development. Data exploration indicated a potential interaction between SST and location; however, when including this interaction, the models failed to converge and thus the term was omitted from the analysis. Models were built with and without S4 to determine sensitivity of model results to the short deployment duration. Excluding this individual did not influence overall model results, and thus it was kept in the final model. Although the saturated model showed all fixed covariates were significant, model selection indicated the mean hourly depth of the animal was best explained by location and individual random effect (Table 3). Unfortunately, there is no established way to calculate the variance explained for individual covariates in GAMMs (Wood, 2006; Zuur *et al.*, 2009).
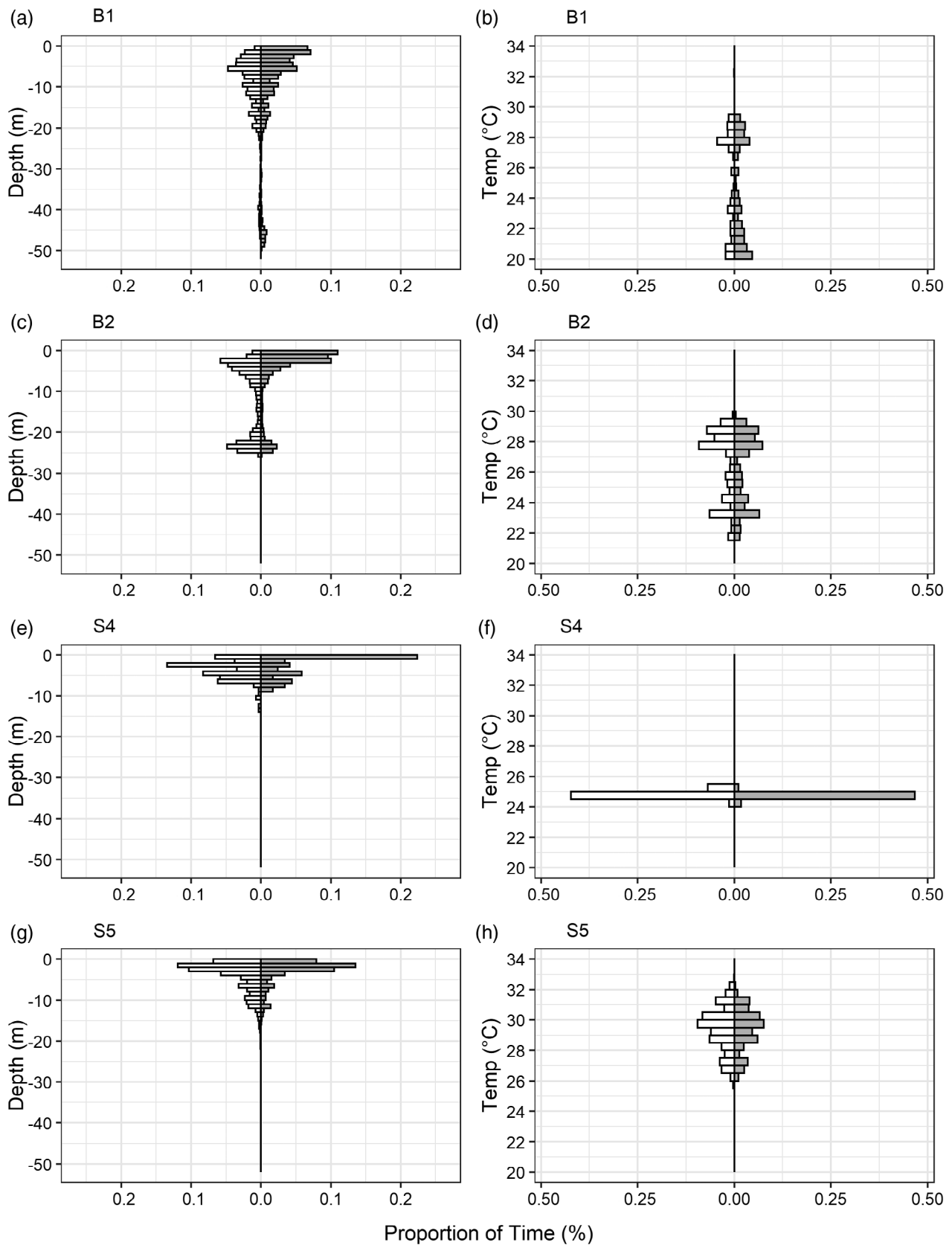
FIGURE 4 Proportion of time each ray spent at depth (1 m bins) and temperature (0.5°C bins) during night (grey) and day (white): B1 (a, e), B2 (b, f), S4 (c, g), S5 (d, h). "Night" is designated as the time between daily sunset and sunrise times at the respective release locations, obtained from the "suncalc" package

TABLE 3 Results of the optimal generalized additive mixed model (gamma distribution) investigating mean hourly depth of *A. narinari*

Covariate	Level	Coefficient	Standard error	t value	P	R² (adj.)
Location	Intercept (Bermuda)	2.17049	0.06289	34.513	<0.01	0.0808
	Sarasota	−0.85104	0.11596	−7.339	<0.01	

TABLE 4 Top five most suitable generalized additive mixed models for investigating mean hourly depth of *A. narinari* in response to the chosen covariates

Model	Intercept	d.f.	Log-likelihoods	AIC	ΔAIC
factor(Location)	**2.170**	**5**	**−3606.887**	**7223.8**	**0.00**
Null	1.803	4	−3610.584	7229.2	5.39
factor(Location) + s(Moon Phase)	2.179	6	−3644.929	7301.9	78.09
s(Moon Phase)	1.787	5	−3659.377	7328.8	104.98
factor(Location) + s(SST)	2.007	7	−3657.563	7329.1	105.36

Note: AIC, Akaike Information Criterion; d.f., degrees of freedom.
All models included ray ID as a random effect and an autocorrelation structure to account for temporal correlation in the data. Bolded model indicates the optimal model.

However, model selection on an exploratory model without a random effect suggested that all covariates should be retained, thus indicating the random effect accounts for most of the model variance. There was substantial evidence for location and individual random effect (ΔAIC = 78.09) as the optimal model over alternative GAMMs with other fixed covariates (Table 4).

The K-S test indicated depth distribution was significantly different between day and night for each animal, with individuals spending a higher proportion of time in deeper water during the day (Figure 4) and depth distribution contracting for B1, B2 and S5 during night hours (Figure S1). Whilst SST—like moon phase and hour of the day—was not included in the optimal model, there was a trend (particularly for the Bermuda rays) towards occupying shallower depths as temperatures rose (Figure S1). The relationship between depth and moon phase was less clear than that of depth and hour of the day, with no clear trend across individuals (Supporting Information Figure S3).

3.2 | Temperature distributions

Collectively, *A. narinari* experienced a temperature range of 18.10–32.86°C (Table 2 and Figure 4). B1 experienced the widest temperature range spanning 14.40°C, encompassing the 10.5°C range obtained by B2 (Table 2). The warmest temperature (32.86°C) was experienced by S5; there was no overlap in temperature range between S4 and S5 (Table 2). Rays experienced cooler temperatures at night, with a collective mean night-time temperature of 26.03°C (±2.38 S.D.) *versus* 26.30°C (±2.22 S.D.) during the day; mean night–day temperature differences ranged from 0.06°C to 0.63°C across individuals (Table 2 and Figure 4). The K-S tests showed statistical differences between day and night temperature distributions for each individual (B1: $D = 0.11$, $P < 0.001$; B2: $D = 0.09$, $P < 0.001$; S4: $D = 0.27$, $P < 0.001$; S5 $D = 0.06$, $P < 0.001$). Seasonal shifts in water temperature were particularly evident in the longer deployments (Figure 3); SSTs cooled from 32.50°C at the beginning of the

deployment on B1 to 18.90°C at the end, from 32.00°C to 23.20°C for B2 and warmed from 28.02°C to 31.65°C for S5.

4 | DISCUSSION

Off the coast of Sarasota, Florida, and surrounding Bermuda, *A. narinari* show similar diel behavioural patterns in vertical habitat use (Figure 3 and Supporting Information Figure S1). In both locations, the rays spent the majority of their time in the upper 10 m of the water column (Figure 4 and Supporting Information Figure S1). This is consistent with previous studies in Harrington Sound indicating that *A. narinari* prefers shallow (<10 m) habitats (Ajemian *et al.*, 2012). The average depth of Sarasota Bay is ∼2 m and the 10 m depth contour occurs approximately 9 km offshore (Figure 1). Of the four rays monitored in the study, both rays from Sarasota and one of the rays from Bermuda (B2) remained above 26 m for the entire deployment (Table 2). These rays were released in relatively shallow water, either on the continental shelf on the west coast of Florida or in Harrington Sound, Bermuda (Figures 1). Ray B1 recorded a maximum depth of 50.5 m, substantially deeper than any of the other rays (Table 2). Ray B1 was released in Harrington Sound; however, the attached PSAT first transmitted from the open ocean southwest of Bermuda, where the depth is approximately 4000 m (Figure 1). For unknown reasons, the tag transmitted late—107 days after it was released from the animal—and thus is not a reliable indicator of animal location.

There is a high likelihood that in areas with shallow bathymetry, the deepest extent of a ray's dive correlates to the sea floor in that location. Harrington Sound, the capture site of the two Bermuda rays, is a 4.8 km² lagoon with a mean depth of 14.5 m and a maximum depth of ∼26 m at Devil's Hole, a remnant sink hole in the south-southeast corner of the sound (Bates, 2017; Figure 1d). The maximum depth obtained by B2 coincides with that of Devil's Hole and was reached on 57.73% of the monitoring days. Typically between October and May the dissolved oxygen in Devil's Hole is similar to

that at the surface; however, during the summer the bottom 3 m of Devil's Hole usually becomes hypoxic with anoxia occurring in September (Bates, 2017). Based on the capture and first transmission locations, in tandem with the depth profile of the animal (Figure 3b), we suspect B2 may have remained within Harrington Sound throughout the deployment but did not access the deeper depths of Devil's Hole during September when dissolved oxygen concentrations were low. B1 displayed similar depth use patterns as B2 until halfway through the deployment, when it must have made forays off the main terrace (<20 m) onto the fore-reef slope (<50 m) of the Bermuda Platform and beyond. While a previous study tracking this species using SPOT tags found that *A. narinari* travels outside of Harrington Sound to the outer reefs of the platform, this species was not previously observed moving off the Bermuda platform as B1 must have done here in order to obtain its depth of 50.5 m (Table 2 and Figure 1c; Ajemian & Powers, 2014). Dives to the 40–50 m depth range occurred repeatedly between late November and February, suggesting that individuals may move offshore during this period when surface water temperatures are below 23°C.

The optimal model indicated that the depth of *A. narinari* was best described by location and individual variation, with the Bermuda animals occupying significantly deeper mean hourly depths than those tagged off Sarasota (Table 3). This may be explained by the difference in bathymetry of the two locations. Sarasota is located along the Gulf of Mexico coast of Florida, where the continental shelf is wide (up to 320 km), while Bermuda is in the Atlantic Ocean far from the continental shelf (Wilhelm & Ewing, 1972). The Bermuda Islands' unique geomorphology includes a volcanic pedestal of three topographic highs that include offshore banks and seamounts within relatively close proximity (50 km) to inshore sounds and lagoons of the Bermuda platform (Vacher & Rowe, 1997). Thus, deeper depths are more readily accessible to the Bermuda animals than the Sarasota rays. However, it should be noted that as the locations of the individuals were unknown, the depth of the water column at any given depth recording cannot be determined and we cannot confirm that rays were occupying the entirety of the water column available to them.

Although hour of the day was not selected in the optimal model to explain mean hourly depth, in both locations *A. narinari* exhibited a diel pattern of vertical habitat use, spending more time at depth during the day while remaining closer to the surface at night (Figure 4 and Supporting Information Figure S1). However, this was not mutually exclusive, and rays could be found near the surface and at depth during both diel periods. These results are consistent with previous studies. In the Indian River Lagoon, FL, U.S.A. active acoustic tracking revealed individuals spent more time in deeper channels during the day and occupied shallower habitats at night (DeGroot et al., 2020). In Harrington Sound, Bermuda, *A. narinari* was observed predominantly in the upper 10 m of the water column and exhibited a diel shift to deeper waters during the day (Ajemian et al., 2012). In a later study involving SPOT tags at the same site (Ajemian & Powers, 2014), transmissions from these tags correlated both to the diel depth patterns noted in the earlier acoustic study and to the patterns noted in this PSAT study.

This pattern of DVM is also in line with other batoid species. For example, *B. brevicaudata* was found to have a similar diel movement pattern, thought to be related to foraging (Le Port et al., 2008). A possible explanation for the behaviour noted in this study is that *A. narinari*, as a benthic predator known to consume bivalves and gastropods (Ajemian et al., 2012; Serrano-Flores et al., 2019), forages in shallow water at night. These prey prefer shallow water (<2 m) (Arnold et al., 1991) and some species are known to exhibit increased nocturnal activity, which may make them easier to detect (Robson et al., 2010). Whilst foraging during the day can confer an advantage to visual predators like white sharks *Carcharodon carcharias* (Linnaeus 1758) (Huveneers et al., 2015), *A. narinari* may be able to detect buried prey such as bivalves just as easily using other sensory organs, under any light conditions. Smith and Merriner (1985) hypothesized that *R. bonasus* could detect the bioelectric fields molluscs produce, using the ampullae of Lorenzini, or the stream of excurrent water from burrowing bivalves. *B. brevicaudata* is known to detect excurrent water jets from worm burrows and clams to find prey (Montgomery & Skipworth, 1997). Research focused on acquiring direct behavioural observations of *A. narinari*, *via* animal-borne cameras or acceleration data loggers, could be beneficial to clarify whether spatiotemporal patterns in diving observed herein are foraging-related (Hays et al., 2015).

Alternative explanations for patterns of DVM often include predator avoidance and behavioural thermoregulation (Matern et al., 2000). *A. narinari* has several known predators that frequent the Gulf of Mexico and Bermuda [e.g., the tiger shark *Galeocerdo cuvier* (Péron & Lesueur 1822) and the great hammerhead shark *Sphyrna mokarran* (Rüppell 1837) (Chapman & Gruber, 2002; Simpfendorfer et al., 2001)]. *A. narinari* may be exhibiting nektobenthic displacement, occupying deeper depths during the day when they can visually detect these predators and moving to shallower habitats at night to seek refuge and forage. The results of this study suggest that vertical movements are not due to behavioural thermoregulation because mean temperatures were similar between night and day (Table 1). Currently, the thermal sensitivity of *A. narinari* is unknown; further research is needed to determine the importance of temperature on the physiological performance and behaviour of this species.

There were some limitations with the modelling process; currently there is no established way to estimate model fit for GAMMS, preventing quantification of the variance explained by each model term (i.e., individual and location) (Wood, 2006; Zuur et al., 2009). Whilst the autocorrelation structure implemented here largely corrected for the temporal autocorrelation, it is not ideal for handling irregularly spaced data which can occur with satellite tags when not all data is relayed (e.g., B1; Figure 3a). As such, there is the possibility that temporal autocorrelation for this animal may have been underestimated. Additionally, an increased sample size would allow for more explanatory variables to be considered in the model, such as animal size and sex. There is evidence in other fishes, including for the batoid *M. californica*, that depth and temperature preferences change with ontogeny (Hopkins & Cech, 2003) whilst sex has been demonstrated to significantly influence the depth and temperature

distribution of *R. bonasus* whereas diel period did not (Omori & Fisher, 2017). Nevertheless, whilst the sample size is small (*n* = 4) our data indicate the importance of location and individual variation in describing the depth use of *A. narinari* whilst showing that diel patterns may hold across individuals.

The most effective PSAT attachment technique was the through-tail method (Figure 2c). All through-tail tags were retained longer than tags attached by other methods, including one (B1), which popped-up after the pre-programed 180 days but reported late (Table 1). Examination of the tag's tether from S5 revealed that a slipped crimp was the breaking point, suggesting that the attachment method to the ray itself was adequate. This method provides a robust mounting point for tagging to reduce drag without interfering with normal behaviours (*e.g.*, males biting the female's pectoral fins during pre-copulation (McCallister *et al.*, 2020)). Its success in similar species, *B. brevicaudata*, indicated its potential for *A. narinari* (Le Port *et al.*, 2008).

Despite its role in the marine food web and designated status as "Near Threatened" by the IUCN, *A. narinari* remains a seldom studied species (Ajemian & Powers, 2014; Cuevas-Zimbrón *et al.*, 2011; Kyne *et al.*, 2006; Tagliafico *et al.*, 2012). As this species has a range that spans several countries, each with fisheries management policies with varying levels of protection, information on the large-scale movement of this mobile ray and position in the water column is important in planning conservation efforts (Ajemian & Powers, 2014; Serrano-Flores *et al.*, 2019). This study provides the first insights into the vertical habitat use of *A. narinari* in both the Gulf of Mexico and western North Atlantic. It indicates the importance of recognizing that individual variation and location can influence behaviour when determining effective management of this species. Furthermore, it demonstrates that the through-tail method of attaching PSATs to *A. narinari* can yield retention times conducive to quantifying their large-scale movements and migration patterns. To better resolve horizontal movement patterns, future studies could combine passive acoustic telemetry with PSAT technology. Inclusion of acoustic tagging data can reduce the error associated with geolocation estimates (Peel *et al.*, 2020) and provide insight into more fine-scale horizontal movement patterns. Future studies should focus on expanding tagging efforts further south in the Gulf of Mexico and the Caribbean. These areas have fewer protections for *A. narinari* and local fisheries exploit the species (Bassos-Hull *et al.*, 2014; Cuevas-Zimbrón *et al.*, 2011; Serrano-Flores *et al.*, 2019). Movement data in these areas will enable researchers to develop management plans that cater to regional movement patterns, as well as to evaluate connectivity between these exploited regions and protected areas to the north.

AUTHOR CONTRIBUTIONS

L.R.B. and M.J.A. conceived the study. K.B.-H., R.E.H., M.J.A., B.M.W. and M.S. obtained funding. M.J.A., C.D., N.B., K.B.-H. and R.E.H. conducted fieldwork. L.R.B., J.P.T., M.J.A., B.V.C., M.N.B., C.D., J.S.H., L.I.N., S.A.McG., M.P. and E.U.-G. conducted analysis and helped to write the manuscript. All authors provided manuscript edits.

ORCID

Lauran R. Brewster https://orcid.org/0000-0002-9798-4370
Kim Bassos-Hull https://orcid.org/0000-0003-2169-9626
Bradley M. Wetherbee https://orcid.org/0000-0002-3753-8950
Matthew J. Ajemian https://orcid.org/0000-0002-2725-4030

REFERENCES

Ajemian, M. J., & Powers, S. P. (2014). Towed-float satellite telemetry tracks large-scale movement and habitat connectivity of myliobatid stingrays. *Environmental Biology of Fishes*, 97, 1067–1081.

Ajemian, M. J., Powers, S. P., & Murdoch, T. J. T. (2012). Estimating the potential impacts of large mesopredators on benthic resources: Integrative assessment of spotted eagle ray foraging ecology in Bermuda. *PLoS One*, 7, e40227.

Akaike, H. (1973). Information theory and an extension of the maximum likelihood principle. In B. N. Petrov, & F. Csaki (Eds.), *Proceedings of the 2nd International Symposium on Information Theory* (pp. 268–281). Publishing House of the Hungarian Academy.

Andrzejaczek, S., Chapple, T. K., Curnick, D. J., Carlisle, A. B., Castleton, M., Jacoby, D. M. P., ... Block, B. A. (2020). Individual variation in residency and regional movements of reef manta rays Mobula alfredi in a large marine protected area. *Marine Ecology Progress Series*, 639, 137–153.

Andrzejaczek, S., Gleiss, A. C., Jordan, L. K. B., Pattiaratchi, C. B., Howey, L. A., Brooks, E. J., & Meekan, M. G. (2018). Temperature and the vertical movements of oceanic whitetip sharks, *Carcharhinus longimanus. Scientific Reports*, 8, 8351.

Andrzejaczek, S., Gleiss, A. C., Lear, K. O., Pattiaratchi, C. B., Chapple, T. K., & Meekan, M. G. (2019). Biologging tags reveal links between fine-scale horizontal and vertical movement behaviors in tiger sharks (*Galeocerdo Cuvier*). *Frontiers in Marine Science*, 6, 229.

Arnold, W. S., Marelli, D. C., Bert, T. M., Jones, D. S., & Quitmyer, I. R. (1991). Habitat-specific growth of hard clams *Mercenaria mercenaria* (L.) from the Indian River, Florida. *Journal of Experimental Marine Biology and Ecology*, 147, 245–265.

Bassos-Hull, K., Wilkinson, K. A., Hull, P. T., Dougherty, D. A., Omori, K. L., Ailloud, L. E., ... Hueter, R. E. (2014). Life history and seasonal occurrence of the spotted eagle ray, *Aetobatus narinari*, in the eastern Gulf of Mexico. *Environmental Biology of Fishes*, 97, 1039–1056.

Bates, N. R. (2017). Twenty years of marine carbon cycle observations at Devils Hole Bermuda provide insights into seasonal hypoxia, coral reef calcification, and ocean acidification. *Frontiers in Marine Science*, 4, 36.

Braun, C. D., Skomal, G. B., Thorrold, S. R., & Berumen, M. L. (2014). Diving behavior of the reef manta ray links coral reefs with adjacent deep pelagic habitats. *PLoS One*, 9, e88170.

Braun, C. D., Skomal, G. B., Thorrold, S. R., & Berumen, M. L. (2015). Movements of the reef manta ray (*Manta alfredi*) in the Red Sea using satellite and acoustic telemetry. *Marine Biology*, 162, 2351–2362.

Brett, J. (1971). Energetic responses of salmon to temperature. A study of some thermal relations in the physiology and freshwater ecology of sockeye salmon (Oncorhynchus Nerkd). *American Zoologist*, 11, 99–113.

Brunnschweiler, J. M., Queiroz, N., & Sims, D. W. (2010). Oceans apart? Short-term movements and behaviour of adult bull sharks *Carcharhinus leucas* in Atlantic and Pacific oceans determined from pop-off satellite archival tagging. *Journal of Fish Biology*, 77, 1343–1358.

Burnham, K. P., & Anderson, D. R. (2002). *Model selection and multimodel inference. A practical information–theoretic approach* (2nd ed.). New York: Springer.

Cerutti-Pereyra, F., Bassos-Hull, K., Arvizu-Torres, X., Wilkinson, K. A., García-Carrillo, I., Perez-Jimenez, J. C., & Hueter, R. E. (2018). Observations of spotted eagle rays (*Aetobatus narinari*) in the Mexican Caribbean using photo-ID. *Environmental Biology of Fishes*, 101, 237–244.

Chapman, D. D., & Gruber, S. H. (2002). A further observation of the prey-handling behavior of the great hammerhead shark, *Sphyrna mokarran*: Predation upon the spotted eagle ray, *Aetobatus narinari*. *Bulletin of Marine Science*, 70, 947–952.

Cooke, S. J. (2008). Biotelemetry and biologging in endangered species research and animal conservation: Relevance to regional, national, and IUCN red list threat assessments. *Endangered Species Research*, 4, 165–185.

Cooke, S. J., Hinch, S. G., Lucas, M. C., & Lutcavage, M. (2012). Biotelemetry and biologging. In A. V. Zale, D. L. Parrish, & T. Sutton (Eds.), *Fisheries techniques* (pp. 819–860). Bethesda, MD: American Fisheries Society.

Cuevas-Zimbrón, E., Pérez-Jiménez, J. C., & Méndez-Loeza, I. (2011). Spatial and seasonal variation in a target fishery for spotted eagle ray *Aetobatus narinari* in the southern Gulf of Mexico. *Fisheries Science*, 77, 723–730.

DeGroot, B., Roskar, G., Brewster, L., & Ajemian, M. (2020). Fine-scale movement and habitat use of whitespotted eagle rays *Aetobatus narinari* in the Indian River Lagoon. *Endangered Species Research*, 42, 109–124.

DeGroot, B. C. (2018). *Movement and habitat use of whitespotted eagle rays, Aetobatus narinari, throughout Florida*, Boca Raton, FL: Florida Atlantic University.

Dewar, H., Mous, P., Domeier, M., Muljadi, A., Pet, J., & Whitty, J. (2008). Movements and site fidelity of the giant manta ray, *Manta birostris*, in the Komodo Marine Park, Indonesia. *Marine Biology*, 155, 121–133.

Flowers, K. I., Henderson, A. C., Lupton, J. L., & Chapman, D. D. (2017). Site affinity of whitespotted eagle rays *Aetobatus narinari* assessed using photographic identification. *Journal of Fish Biology*, 91, 1337–1349.

Galuardi, B. (2012). Analyzepsat: Functions for Microwave Telemetry PSAT Analysis.

Grusha, D. S. (2005). *Investigation of the life history of the cownose ray, Rhinoptera bonasus (Mitchill 1815)*, Gloucester Point, VA: . College of William and Mary - Virginia Institute of Marine Science.

Hastie, T., & Tibshirani, R. (1990). Generalized additive models. In *Encyclopedia of statistical sciences*. Boca Raton, FL: John Wiley & Sons, Inc.

Hays, G. C. (2015). New insights: animal-borne cameras and accelerometers reveal the secret lives of cryptic species. *Journal of Animal Ecology*, 84(3), 587–589.

Hays, G. C., Ferreira, L. C., Sequeira, A. M. M., Meekan, M. G., Duarte, C. M., Bailey, H., … Thums, M. (2015). Key questions in marine megafauna movement ecology. *Trends in Ecology & Evolution*, 31, 463–475.

Hopkins, T. E., & Cech, J. J. (2003). The influence of environmental variables on the distribution and abundance of three elasmobranchs in Tomales Bay, California. *Environmental Biology of Fishes*, 66, 279–291.

Hueter, R. E., Tyminski, J. P., Pina-Amargós, F., Morris, J. J., Abierno, A. R., Valdés, J. A. A., & Fernández, N. L. (2018). Movements of three female silky sharks (*Carcharhinus falciformis*) as tracked by satellite-linked tags off the Caribbean coast of Cuba. *Bulletin of Marine Science*, 94, 345–358.

Humphries, N. E., Simpson, S. J., & Sims, D. W. (2017). Diel vertical migration and central place foraging in benthic predators. *Marine Ecology Progress Series*, 582, 163–180.

Hussey, N. E., Kessel, S. T., Aarestrup, K., Cooke, S. J., Cowley, P. D., Fisk, A. T., … Whoriskey, F. G. (2015). Aquatic animal telemetry: a panoramic window into the underwater world. *Science*, 348, 1255642.

Huveneers, C., Holman, D., Robbins, R., Fox, A., Endler, J. A., & Taylor, A. H. (2015). White sharks exploit the sun during predatory approaches. *The American Naturalist*, 185, 562–570.

Kyne, P. M., Ishihara, H., Dudley, S. F. J., & White, W. T. (2006). *Aetobatus narinari*. IUCN red list of threatened species 2006, doi:https://doi.org/10.2305/IUCN.UK.2006.RLTS.T39415A10231645.en

Le Port, A., Sippel, T., & Montgomery, J. C. (2008). Observations of mesoscale movements in the short-tailed stingray, *Dasyatis brevicaudata* from New Zealand using a novel PSAT tag attachment method. *Journal of Experimental Marine Biology and Ecology*, 359, 110–117.

Matern, S. A., Cech, J. J., & Hopkins, T. E. (2000). Diel movements of bat rays, *Myliobatis californica*, in Tomales Bay, California: Evidence for behavioral thermoregulation? *Environmental Biology of Fishes*, 58, 173–182.

McCallister, M., Mandelman, J., Bonfil, R., Danylchuk, A., Sales, M., & Ajemian, M. (2020). First observation of mating behavior in three species of pelagic myliobatiform rays in the wild. *Environmental Biology of Fishes*, 103, 163–173.

Montgomery, J., & Skipworth, E. (1997). Detection of weak water jets by the short-tailed stingray *Dasyatis brevicaudata* (Pisces: Dasyatidae). *Copeia*, 1997, 881.

Naylor, G. J. P., Caira, J. N., Jensen, K., Rosana, K. A. M., White, W. T., & Last, P. R. (2012). A DNA sequence–based approach to the identification of shark and ray species and its implications for global elasmobranch diversity and parasitology. *Bulletin of the American Museum of Natural History*, 367, 1–262.

Nielson, A., Sibert, J., Ancheta, J., Galuardi, B., & Lam, C. H. (2009). *Ukfsst: Kalman filter tracking including sea surface temperature*.

Omori, K. L., & Fisher, R. A. (2017). Summer and fall movement of cownose ray, *Rhinoptera bonasus*, along the east coast of United States observed with pop-up satellite tags. *Environmental Biology of Fishes*, 100, 1435–1449.

O'Shea, O. R., Thums, M., van Keulen, M., & Meekan, M. (2012). Bioturbation by stingrays at Ningaloo Reef, Western Australia. *Marine and Freshwater Research*, 63, 189.

Peel, L. R., Stevens, G. M. W., Daly, R., Daly, C. A. K., Collin, S. P., Nogués, J., & Meekan, M. G. (2020). Regional movements of reef manta rays (Mobula Alfredi) in Seychelles waters, 7, 1–17.

R Core Team (2020). *R: A language and environment for statistical computing*. Vienna, Austria: R Foundation for Statistical Computing. Retrieved from https://www.R-project.org/.

Richards, V. P., Henning, M., Witzell, W., & Shivji, M. S. (2009). Species delineation and evolutionary history of the globally distributed spotted eagle ray (*Aetobatus narinari*). *Journal of Heredity*, 100, 273–283.

Robson, A. A., de Leaniz, C. G., Wilson, R. P., & Halsey, L. G. (2010). Effect of anthropogenic feeding regimes on activity rhythms of laboratory mussels exposed to natural light. *Hydrobiologia*, 655, 197–204.

Sellas, A. B., Bassos-Hull, K., Pérez-Jiménez, J. C., Angulo-Valdés, J. A., Bernal, M. A., & Hueter, R. E. (2015). Population structure and seasonal migration of the spotted eagle ray, *Aetobatus narinari*. *Journal of Heredity*, *106*, 266–275.

Sequeira, A. M. M., Heupel, M. R., Lea, M. A., Eguíluz, V. M., Duarte, C. M., Meekan, M. G., ... Hays, G. C. (2019). The importance of sample size in marine megafauna tagging studies. *Ecological Applications*, *29*, 1–17.

Serrano-Flores, F., Pérez-Jiménez, J. C., Méndez-Loeza, I., Bassos-Hull, K., & Ajemian, M. J. (2019). Comparison between the feeding habits of spotted eagle ray (*Aetobatus narinari*) and their potential prey in the southern Gulf of Mexico. *Journal of the Marine Biological Association of the United Kingdom*, *99*, 661–672.

Silliman, W., & Gruber, S. H. (1999). Behavioral biology of the spotted eagle ray, *Aetobatus narinari* (Euphrasen, 1790), in Bimini Bahamas; an interim report. *Bahamas Journal of Science*, *7*, 13–20.

Simpfendorfer, C. A., Goodreid, A. B., & Mcauley, R. B. (2001). Size, sex and geographic variation in the diet of the tiger shark, *Galeocerdo Cuvier*, from Western Australian waters. *Environmental Biology of Fishes*, *61*, 37–46.

Smith, J. W., & Merriner, J. V. (1985). Food habits and feeding behavior of the cownose ray, *Rhinoptera bonasus*, in lower Chesapeake Bay. *Estuaries*, *8*, 305–310.

Tagliafico, A., Rago, N., Rangel, S., & Mendoza, J. (2012). Exploitation and reproduction of the spotted eagle ray (*Aetobatus narinari*) in the Los Frailes Archipelago, Venezuela. *Fishery Bulletin*, *110*, 307–316.

Thieurmel, G., & Elmarhraoui, A. (2019). Package 'Suncalc': Compute sun position, sunlight phases, moon position and lunar phase. R package version 0.5. 2019.

Vacher, H. L., & Rowe, M. P. (1997). Geology and hydrogeology of Bermuda. In H. L. Vacher & T. Quinn (Eds.), *Geology and hydrology of carbonate islands* (pp. 35–90). Amsterdam: Elsevier.

Vaudo, J. J., Wetherbee, B. M., Harvey, G., Nemeth, R. S., Aming, C., Burnie, N., ... Shivji, M. S. (2014). Intraspecific variation in vertical habitat use by tiger sharks (*Galeocerdo Cuvier*) in the western North Atlantic. *Ecology and Evolution*, *4*, 1768–1786.

Vianna, G. M. S., Meekan, M. G., Meeuwig, J. J., & Speed, C. W. (2013). Environmental influences on patterns of vertical movement and site fidelity of grey reef sharks (*Carcharhinus amblyrhynchos*) at aggregation sites. *PLoS One*, *8*, e60331.

Ward, C. R. E., Bouyoucos, I. A., Brooks, E. J., & O'Shea, O. R. (2019). Novel attachment methods for assessing activity patterns using triaxial accelerometers on stingrays in the Bahamas. *Marine Biology*, *166*, 1–8.

Wearmouth, V. J., & Sims, D. W. (2009). Movement and behaviour patterns of the critically endangered common skate *Dipturus batis* revealed by electronic tagging. *Journal of Experimental Marine Biology and Ecology*, *380*, 77–87.

White, W., Last, P., Naylor, G., K, J., & Caira, J. (2010). *Clarification of Aetobatus ocellatus (Kuhl, 1823) as a valid species, and a comparison with Aetobatus narinari (Euphrasen, 1790) (Rajiformes: Myliobatidae)* (CSIRO Marine and Atmospheric Researsh Paper, 32) (pp. 141–164). Tasmania.

Whitty, J. M., Keleher, J., Ebner, B. C., Gleiss, A. C., Simpfendorfer, C. A., & Morgan, D. L. (2017). Habitat use of a critically endangered elasmobranch, the largetooth sawfish *Pristis pristis*, in an intermittently flowing riverine nursery. *Endangered Species Research*, *34*, 211–227.

Wilhelm, O., & Ewing, M. (1972). Geology and history of the Gulf of Mexico. *GSA Bulletin*, *83*, 575–600.

Wood, S. N. (2006). *Generalized additive models. An introduction with R.* Boca Raton, FL: Chapman Hall/CRC.

Zuur, A. F., Ieno, E. N., & Elphick, C. S. (2010). A protocol for data exploration to avoid common statistical problems. *Methods in Ecology and Evolution*, *1*, 3–14.

Zuur, A. F., Ieno, E. N., Walker, N. J., Saveliev, A. A., & Smith, G. M. (2009). *Mixed effects models and extensions in ecology with R.* New York: Springer Science+Business Media.

SUPPORTING INFORMATION

Additional supporting information may be found online in the Supporting Information section at the end of this article.